PAPER

Check for updates

Cyclopenta-fused polyaromatic hydrocarbons: synthesis and characterisation of a stable, carbon-centred helical radical†

Stefan Herzog, [ID] [a] Alexander Hinz, [ID] *[b] Frank Breher [ID] *[b] and Joachim Podlech [ID] *[a]

An air- and moisture-stable helical radical with seven six- and five-membered rings arranged alternately was synthesized by cyclizations in a suitably *ortho,ortho'*-substituted terphenyl and re-establishment of its conjugation. Mesityl groups at the five-membered rings prevent radical reactions. This cyclopenta-fused polyaromatic hydrocarbon (CP-PAH) was characterized by X-ray crystallographic analysis, EPR and UV/Vis spectroscopy, and by cyclic voltammetry. Further properties and spectra were determined by quantum chemical calculation (spin densities, orbital energies, UV/Vis/NIR and ECD spectra). It turned out that this radical is best described with its radical centre being in the outer five-membered rings, which allows for the largest number of fully intact benzene rings. Its triradical character is rather small and can be neglected. The five-membered rings show significant antiaromatic character, which is highest in the central ring.

Introduction

π-Conjugated polycyclic hydrocarbons (PHs),[1] in which six- and five-membered rings are arranged alternately, have been referred to as cyclopenta-fused polyaromatic hydrocarbons (CP-PAHs),[2] as non-alternant conjugated polycyclic hydrocarbons (CPHs),[3] or as compounds with quinoidal conjugated units.[4] Substrates with five or nine rings are occasionally only termed with their rational names as indenofluorenes (IFs)[5] and indacenodifluorenes (IDFs),[1f,2a,6] respectively. A selection of representatives (**1**–**3**) with roughly linear structure is given in Fig. 1. Depending on the specific fusion, the number of rings, and the maximum number of fully intact benzene rings (Clar's rule[7]) in the respective resonance structures, these compounds show either a closed shell behaviour (*e.g.*, **1A**), di- or tetraradical character (*e.g.*, **3B**), or are radicals (*e.g.* **2A**). Decomposition and side reactions[8] based on possibly emerging radical properties are typically avoided by attachment of bulky aryl groups at specific positions (*e.g.*, of mesityl groups,

Mes), usually at the five-membered rings.[9] A number of unique electronic (*e.g.*, small HOMO–LUMO gaps), optical, and magnetic properties have been associated with these compounds, which could possibly lead to applications in organic electronics,[1g,10] in spintronics, and non-linear optics,[11] and might be used for energy storage.[1f]

While CP-PAHs with two or four five-membered rings can either be given with closed shell resonance structures or with di- or tetraradical structures (*e.g.*, **1**, **3**),[1f,12] the CP-PAHs with three five-membered rings (*e.g.*, **2**) are necessarily radicals and thus need to possess an open-shell configuration. Neither of the 21 supposable unbranched compounds with seven rings (*e.g.*, **2**; all possible structures are given in the ESI†) seems to have been synthesized yet, but a branched truxene derivative **4** with a presumed triradical structure has been synthesized and investigated.[13] These and similar persistent organic radicals and diradicals[9b,d,14] are of significant interest due to their redox properties, their possible application as electrode-active materials,[15] and their magnetic behavior.[16]

CP-PAHs with two helical arms (**5** and **6**, which are given in Fig. 1 with their closed shell configuration) have similarly been synthesized and investigated.[6,12d] These compounds turned out to be achiral and adopt *meso* structures. According to the IUPAC definition, helicenes are *ortho*-fused polycyclic aromatic or heteroaromatic compounds in which all rings (minimum five) are angularly arranged so as to give helically shaped molecules, which are thus chiral,[17] while according to a more recent statement of the IUPAC, the term helicene might only be applicable to systems with at least six *ortho*-

[a]Institut für Organische Chemie, Karlsruher Institut für Technologie (KIT), 76131 Karlsruhe Fritz-Haber-Weg 6, Germany
[b]Institut für Anorganische Chemie, Karlsruher Institut für Technologie (KIT), 76131 Karlsruhe Engesserstraße 15, Germany. E-mail: breher@kit.edu, alexander.hinz@kit.edu

†Electronic supplementary information (ESI) available: Experimental procedures, copies of ^{1}H and ^{13}C NMR spectra for all new compounds, further characterisation data of **7**, computational details. CCDC 2129930. For ESI and crystallographic data in CIF or other electronic format see https://doi.org/10.1039/d2ob00172a
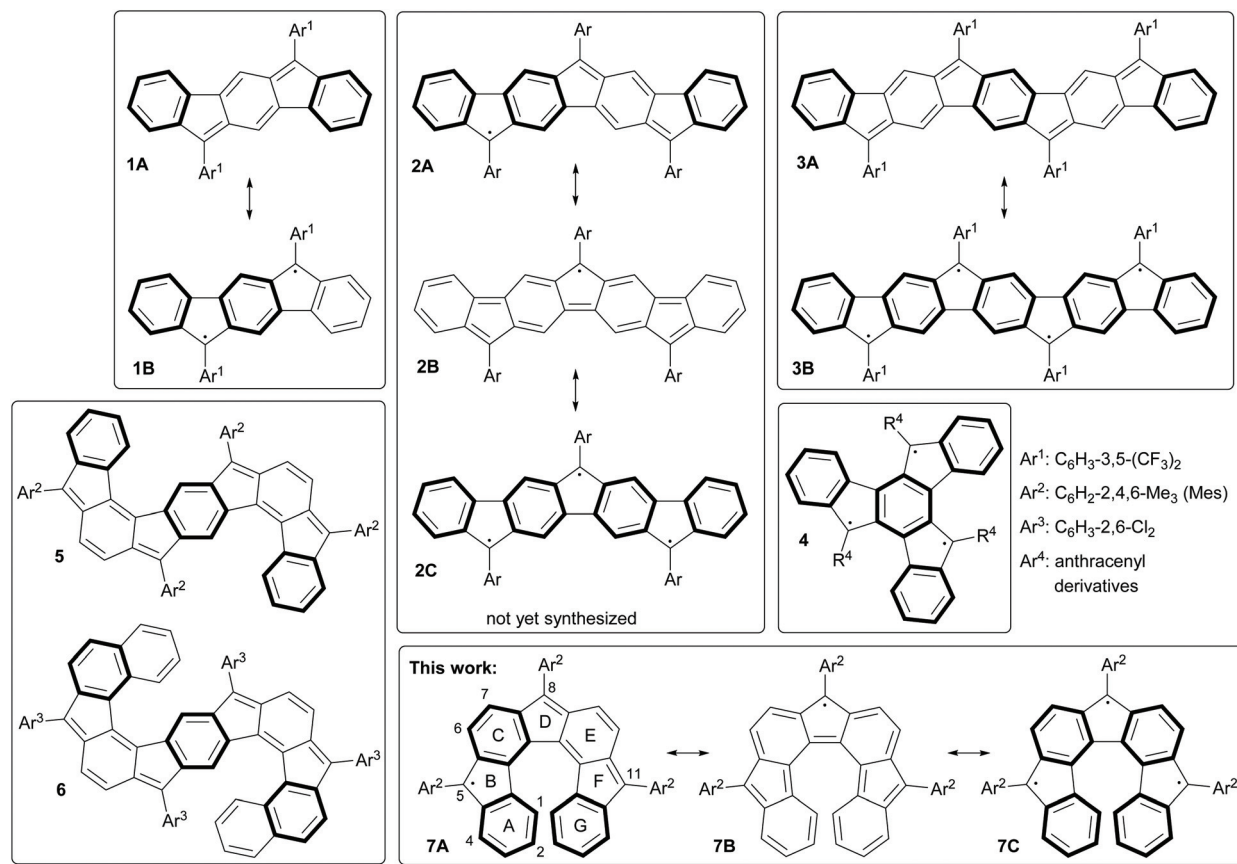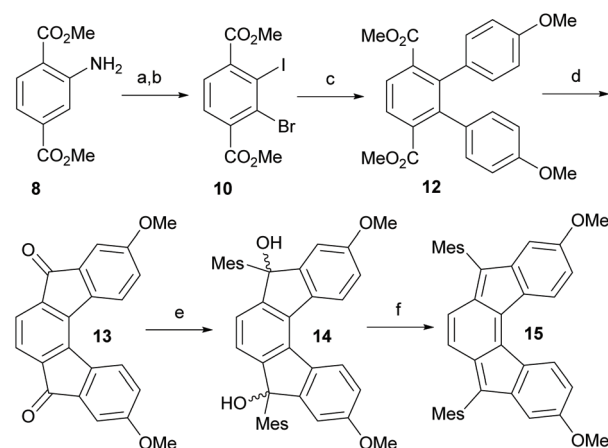
This journal is © The Royal Society of Chemistry 2022

Org. Biomol. Chem., 2022, **20**, 2873–2880 | **2873**

Fig. 1 A selection of CP-PAHs containing two, three, or four five-membered rings. Fully benzoid rings are highlighted in bold.

fused rings.[18] While non-conjugated[19] or cationic[20] helicenes containing five-membered rings have already been synthesized, no report came to our attention dealing with chiral CP-PAH helicenes (e.g., 7). Herein we present the synthesis of helical CP-PAHs, for which the above-mentioned properties might be supplemented by chiroptic properties.

Synthesis of helical CP-PAHs

We recently developed a method in which the fusion of ortho, ortho'-substituted terphenyls yielded [5]helicene-type compounds[21] and we considered this strategy suitable for the construction of even larger helicenes by using similarly substituted quaterphenyls or even higher oligophenyls. We envisioned the synthesis of helical CP-PAHs with this method and at first aimed for a helicene with five rings (containing two five-membered rings). These compounds have already been prepared, albeit via differing routes.[1k,6,22] We started this endeavour with purchasable dimethyl 2-aminoterephthalate 8, which was brominated with N-bromosuccinimide (NBS) and then subjected to a Sandmeyer reaction yielding the dihalogenated diester 10 (Scheme 1). Double Suzuki coupling with 2-(4-methoxyphenyl)-4,4,5,5-tetramethyl-1,3,2-dioxaborolane 11[23] and double intramolecular Friedel–Crafts-type reaction using Eaton's reagent (a solution of phosphorus pentoxide in methanesulfonic acid)[24] furnished the [5]helicene-type compound
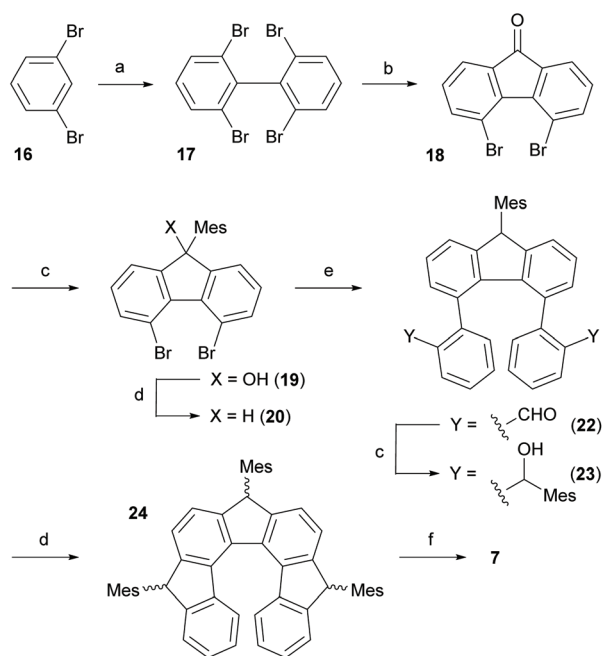

Scheme 1 Synthesis of indeno[2,1-c]fluorene 15. Conditions: (a) NBS, AcOH, toluene, rt, 4 d (→ 9, 29%); (b) NaNO$_2$, aq. HCl, then KI, 0 °C to rt, 17 h (68%); (c) MeOC$_6$H$_4$Bpin (11), cat. Pd(PPh$_3$)$_2$Cl$_2$, Na$_2$CO$_3$, THF/H$_2$O (1 : 1), 80 °C, 15 h (61%); (d) P$_4$O$_{10}$ in MeSO$_3$H (7.7%, w/w; Eaton's reagent), 80 °C, 15 h (52%); (e) MesLi, THF, −78 °C to rt, 2.5 h (not isolated); (f) SnCl$_2$, TFA, toluene, 50 °C, 16 h (49%, 2 steps).

13. Double addition of mesityllithium yielded diol 14 as a mixture of stereoisomers. 14 was not isolated but immediately reduced with tin(ɪɪ) chloride in trifluoroacetic acid (TFA)[22] to the fully conjugated CP-PAH [5]helicene 15. The methoxy

2874 | Org. Biomol. Chem., 2022, 20, 2873–2880

This journal is © The Royal Society of Chemistry 2022

groups were used to facilitate the detection during chromatographic purification of the intermediates, to simplify analysis of the ^{1}H NMR spectra, and to promote the intramolecular S_EAr reactions. Later on (*vide infra*) it turned out that the methoxy groups are not necessary and were thus not used in further investigations. Since CP-PAH [5]helicenes very similar to **15** have already been synthesized *via* different routes and have been investigated thoroughly (including the measuring of UV/Vis spectra and cyclic voltammograms),[1k,6,22] we did not aim for further representatives but turned to higher helicenes of this type.

Helicene **7** was synthesized using a similar strategy starting with 1,3-dibromobenzene (**16**), which was converted to tetrabromobiphenyl **17**[25] and subjected to a halogen-metal exchange in the presence of methyl chlorocarbonate to yield fluorenone **18** (Scheme 2). Addition of mesitylmagnesium bromide and subsequent reduction of the alcohol group with triethylsilane furnished dibromide **20**, which could be coupled with *ortho*-formylated phenylboronic acid pinacol ester **21**[26] in a double Suzuki reaction. Both formyl groups are again reacted with a mesityl Grignard reagent, treated with boron trifluoride, and oxidized with tetrachloro-*p*-benzoquinone yielding [7]helicene-type CP-PAH **7**. Its synthesis was completed starting with 1,3-dibromobenzene (**16**) in 8 steps with a total yield of 2.3%.

Scheme 2 Synthesis of helicene-type radical **7**. Conditions: (a) 1. LDA, THF, −78 °C to rt, 20 h; 2. CuCN, LiCl; 3. benzoquinone (29%); (b) BuLi, ClCO$_2$Me, THF, −78 °C, 3 h (74%); (c) MesMgBr, THF, 0 °C to rt, 20 h (**19**: 70%, **23**: not isolated); (d) BF$_3$·OEt$_2$, Et$_3$SiH, CH$_2$Cl$_2$, 0 °C, 1 h (**20**: 71%, **24**: (no Et$_3$SiH added) mixture of isomers, 61%, two steps); (e) *o*-formyl-C$_6$H$_4$Bpin (**21**), Na$_2$CO$_3$, cat. PdCl$_2$(PPh$_3$)$_2$, THF/H$_2$O (1:1), 80 °C, 15 h (mixture of isomers, 43%); (f) *t*BuOK, THF, 60 °C, 16 h, then tetrachloro-*p*-benzoquinone, rt, 5 min (84%).

Characterization of helical radical 7

The carbon-centred helical radical **7** is a moisture- and air-stable solid that appears green in solution. It was subjected to a liquid/liquid diffusion in a chloroform/ethanol solvent system and furnished very dark, virtually black crystals suitable for X-ray crystallographic analysis (Fig. 2).† The two independent molecules in the unit cell show slightly differing geometries (what is relevant for determination of the HOMA values, *vide infra*). The most relevant difference between both molecules lies in the angles between the planes of terminal rings A and G, which differ by 11.0° and thus highlight some flexibility of the helix. The mesityl groups deviate from the planes perpendicular to the respective cyclopentane planes by 9 to 25°. These distortions are in line with the findings from the vibrational analysis (see ESI†), showing that a twisting of the mesityl groups is found at frequencies around 10–15 cm^{-1}, *i.e.* at very low energies. **7** crystallizes in the space group $P2_1/c$ and the racemic crystal is composed of both helical enantiomers. Details to the crystallographic analysis are given in the ESI.† The thus obtained crystals show a melting behaviour at 514 K. At this point the crystals seem to lose solvent and keep their solid character. No further phase transition was observed until about 620 K.

Clean NMR spectra could be measured from [5]helicene **15**, while it shows no EPR signal. This clearly confirms its closed-shell configuration, what has already been noted previously.[22]

[7]Helicene **7**, on the other hand, gave no NMR spectra and a singlet resonance with no discernible hyperfine structure at g = 2.0013 was detected by X-band EPR spectroscopy (Fig. 3).[27] According to computed hyperfine coupling constants (see ESI†) nearly all protons contribute in the same order of magnitude which corroborates the experimentally observed singlet resonance with no resolved multiplet but a broadened line instead ($\omega_{1/2}$ = 0.8 mT). No decay of the EPR resonance of a sample in oxygen-saturated toluene could be observed over time.

The aromaticity of a CP-PAH (*i.e.* its aromatic or antiaromatic character) is correlated with its HOMO–LUMO gap being of great importance for its electronic properties. Standard pro-
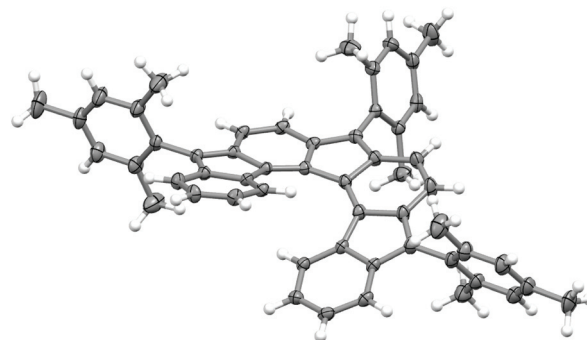

Fig. 2 A projection of the molecular structure of compound **7**. Only one of the crystallographically independent molecules is shown. (Thermal ellipsoids are depicted at the 30% probability level.).†
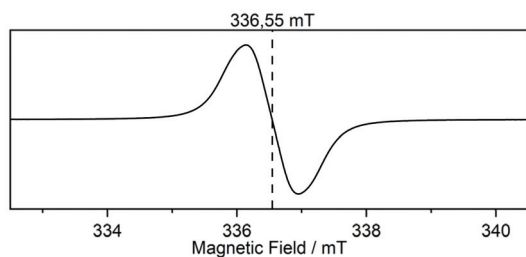
Fig. 3 EPR spectrum of **7** at X-band (9.427 GHz) at room temperature in toluene.

cedures for its evaluation are determination of HOMA values (harmonic oscillator model of aromaticity),[28] which give the mean deviation from an ideally aromatic non-alternating bond length, and of NICS values (nucleus-independent chemical shift),[29] which give the absolute magnetic shielding, usually calculated at 1 Å distance from the respective ring centre [$NICS_{zz}(1.0)$ values]. Both values are typically determined for each individual ring of a polycyclic compound. HOMA values can be extracted from crystallographic or from calculated data, while NICS values are only obtained from calculations. HOMA values for compound **7** are given in Fig. 4 (left: black numbers from crystallographic data; blue numbers from calculated data); they clearly account for an aromatic character in the outer benzene rings A and G, for a considerably reduced aromaticity in the inner benzene rings C and E, and for a significant antiaromatic character in the five-membered rings. The lowest HOMA values (lowest aromaticity) were determined for the central ring; they are 0.04 and 0.24, respectively. The approach to these values and some values for comparison are given in the ESI.† These findings were supported by the calculated $NICS_{zz}(1.0)$ values (Fig. 4, right): since we suspected some of the values to be obscured by the mesityl groups, we additionally determined all values for the parent compound **25** (R = H). It turned out that the values for both compounds are virtually identical; they are fully in line with the information deduced from the HOMA values: The outer rings A and G show

aromatic behaviour (negative NICS values), the central benzene rings C and E are slightly antiaromatic, while a significant antiaromatic character can be determined for the five-membered rings (the highest positive value again for the central ring D).

The aromatic *vs.* antiaromatic character can furthermore be estimated from ^{1}H NMR spectra since protons at the outer rim are shielded in antiaromatic compounds.[30] While NMR spectra of **7** could not easily[31] be measured due to its paramagnetic behaviour, we were able to calculate magnetic shielding tensors for this compound, which are easily converted into chemical shifts (δ values). Since we suspected the mesityl groups to obscure the shielding, we additionally calculated these values for the parent compound **25**, which furthermore allowed the determination of the NMR-spectroscopic properties of protons at the five-membered rings (see ESI†). Protons 3-H and 4-H (for numbering, see Fig. 1) in **25** have calculated shifts of 7.04 and 7.16 ppm, which is expected for the aromatic ring. However, the protons 5-H, 6-H, 7-H, and 8-H, which are bound to rings with antiaromatic character according to the calculated NICS values, show only slightly upfield-shifted resonances at δ = 6.66, 6.77, 6.62, and 6.43 ppm, respectively. The shifts for protons 1-H and 2-H (6.55, 6.60 ppm) are similarly shifted upfield, possibly due to interactions with the opposite ring G.

A spin density map for **7** is given in Fig. 5. Positions 5 and 11 show Mulliken atomic spin densities of 0.34 each, while the central position 8 carries a spin density of only −0.24 (see ESI†). Since the SOMO shows a nodal plane through the centre of the molecule (*cf.* Fig. 6) and thus through atom C-8, the significant spin density observed at this position is most likely due to negative spin polarization. These findings give evidence for the predominance of the degenerate resonance formulas **7A** (with the radical centres at the peripheral cyclopentane rings) over resonance formula **7B** (where the radical is located in the central ring). This goes in line with Clar's rule, expressing that the most contributing resonance formulas are those with the largest number of fully intact benzene rings.[7] SOMOs
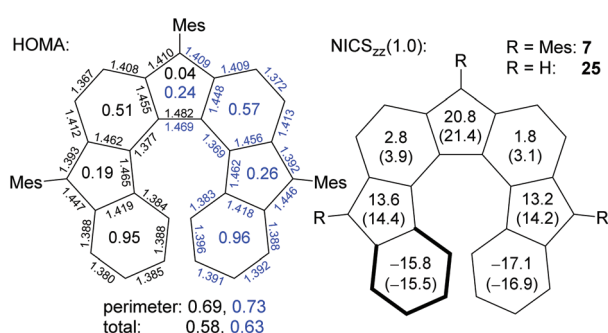

Fig. 4 Left: Bond length of **7** are given at the bonds (black: averaged values from the two roughly C_2-symmetric independent molecules in the unit cell; blue: calculated values). HOMA values are given in the rings. Right: $NICS_{zz}(1.0)$ values for R = Mes (R = H); Dummy atoms were located above the paper plane.
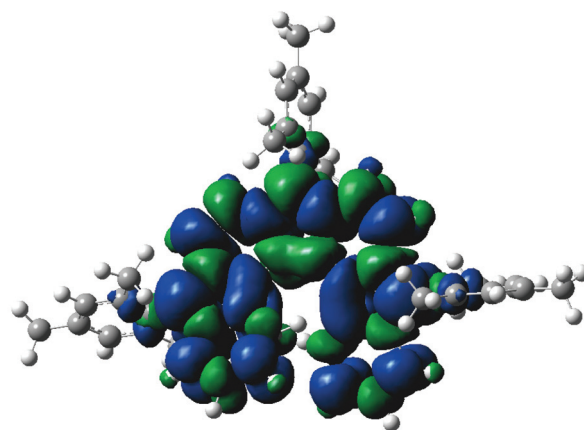

Fig. 5 Calculated spin density of **7**. Blue and green surfaces represent α and β spin density, respectively (isovalue: 0.004 electrons per bohr³).
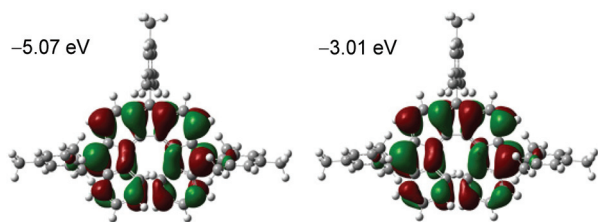
2876 | *Org. Biomol. Chem.*, 2022, **20**, 2873–2880

This journal is © The Royal Society of Chemistry 2022

−5.07 eV   −3.01 eV

Fig. 6 Calculated SOMOs of α and β electrons, respectively, for radical **7** (isovalue: 0.02 electrons$^{1/2}$·bohr$^{-3/2}$).

of radical **7** for both the α and the β electron are given in Fig. 6. More frontier orbitals together with their energies are given in the ESI.† It could be noted that the SOMO and at least the first two HOMOs and LUMOs are MOs essentially build up by the helicene core; the mesityl groups are hardly involved herein.

The electrochemical properties of **7** were determined by cyclic voltammetry (CV, potentials *vs.* the ferrocene/ferrocenium couple, Fc/Fc$^+$); the voltammograms are given in Fig. 7. Four quasi-reversible redox processes were observed in tetrahydrofuran at $E_{1/2}^0$(THF) values of −2.73, −2.15, −1.36, and −0.05 V, while five quasi-reversible redox processes at $E_{1/2}^0$(CH$_2$Cl$_2$) values of −2.14, −1.37, −0.16, +1.11, and +1.55 V were observed in methylene chloride (for further details, see ESI†). The values obtained in CH$_2$Cl$_2$ suggest that three reductions (1–3) and two oxidations (4, 5) are possible for **7**. In addition,
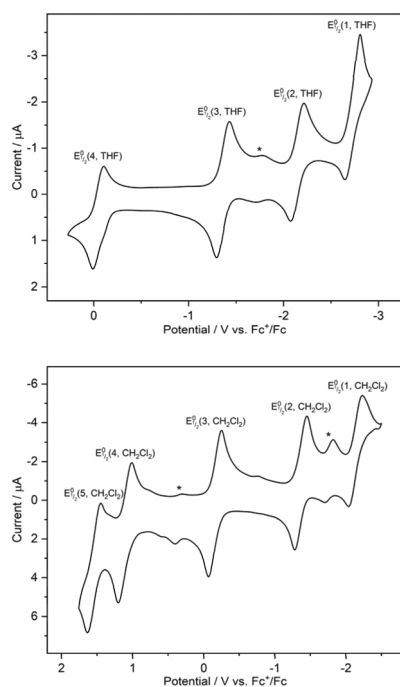

Fig. 7 Cyclic voltammograms of **7** in THF (top) and CH$_2$Cl$_2$ (bottom) measured at room temperature (*vs.* Fc/Fc$^+$; *ν*(THF) = 200 mV s^{-1}, *ν*(CH$_2$Cl$_2$) = 500 mV s^{-1}; Pt/[^{n}Bu$_4$N][Al(OC(CF$_3$)$_3$)$_4$]/Ag). The asterisk marks unidentified electrochemical responses of unknown origin.

an electrochemical SOMO–LUMO gap can be deduced from these values:[32] E_{SOMO}: −(4.8 + $E_{1/2}^0$(4, CH$_2$Cl$_2$)) eV = −(4.8 + 1.11) eV = −5.91 eV; E_{LUMO}: −(4.8 + $E_{1/2}^0$(3, CH$_2$Cl$_2$)) eV = −(4.8 − 0.16) eV = −4.64 eV. The thus obtained gap of 1.27 eV is reasonably close to the optical gap obtained from TD calculations (1.17 eV, *vide infra*). The electrochemical HOMO–SOMO gap might analogously be estimated from the difference of $E_{1/2}^0$(3, CH$_2$Cl$_2$) = −0.16 and $E_{1/2}^0$(2, CH$_2$Cl$_2$) = −1.37 to be 1.21 eV. Nevertheless, it should be noted that electrochemical gaps and even more optical gaps were reported to underestimate the actual gaps to some extent.[32c]

The triradical character of **7** (which would be exemplified by resonance formula **7C**) was determined by natural orbital occupation number (NOON)[33] calculations at the spin unrestricted B3LYP/6-31 g(d,p) level. According to Yamaguchi's scheme[12a,34] the triradical character *y* (see ESI†) was calculated to be only 0.003 and thus to be significantly smaller than the diradical character in, *e.g.*, polycycle **6** (*y* = 0.12).[12d] Calculation at the uCAM-B3LYP/6-31 g(d,p) level (considering long-range correction) resulted in a somewhat higher triradical character (*y* = 0.03). This leads once more to the conclusion that the degenerate resonance formulas **7A** are most significant; the triradical resonance formula **7C** showing three fully intact benzene rings is of minor relevance. The rather small contribution of resonance formula **7B** has already been deduced from the spin densities (*vide supra*).

The singlet/triplet gap is important for closed shell compounds and this might lead analogously to a contingent importance of doublet/quartet gaps in radicals like **7**. The energy difference of these states in helicene **7** was calculated at the uM06/6-311++g(d,p) level to be 83.5 kJ mol^{-1} (0.87 eV), *i.e.*, the state in which three unpaired electrons have the same spin is significantly less stable und might thus be of minor relevance.

UV/Vis/NIR and electronic circular dichroism (ECD) spectra were calculated with a time-dependent (TD) calculation at the uM06/6-311 g(d,p) level applying a modelled dichloromethane solvent field (Fig. 8, bottom). The functional M06 was reported to be well suited for TD calculations.[35] The calculated UV/Vis spectrum of **7** in CH$_2$Cl$_2$ is in good agreement with a measured spectrum (Fig. 8, top; spectra with identical und thus comparable sections and scalings are given in the ESI†). It shows a very weak absorption band at 1056 nm (1.17 eV; oscillator strength *f* = 0.002), induced by the transition from the α-spin SOMO to the LUMO and from the β-spin HOMO−1 to the respective SOMO (see ESI†). This absorption is not visible in the measured UV/Vis/NIR spectrum (see ESI†). A sharp absorption band at 812 nm (*f* = 0.172) is essentially due to α-spin SOMO → LUMO and β-spin HOMO−1 → SOMO transitions. The next significant absorption band (here plotted as a shoulder) at 552 nm (*f* = 0.073) represents mainly α-HOMO−1 → LUMO, β-HOMO−2 → SOMO, and β-HOMO−1 → LUMO transitions. All these transitions are between orbitals fully spread over the helicene's π-system (see ESI†). The dominant transition at 812 nm is also the most significant band in the ECD spectrum.
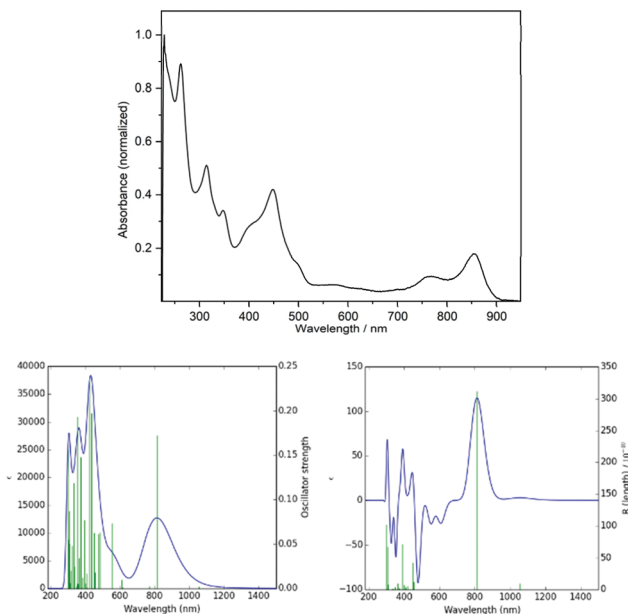
This journal is © The Royal Society of Chemistry 2022

Org. Biomol. Chem., 2022, **20**, 2873–2880 | **2877**

Fig. 8 Measured UV/Vis spectrum of **7** (top) in CH$_2$Cl$_2$. Calculated UV/Vis/NIR (bottom left) and ECD spectra (bottom right).

Conclusion

In summary we synthesized a helical CP-PAH consisting of four benzene and three cyclopentadiene rings which is a further example of a stable carbon-centred radical. It was obtained by cyclization of an *ortho,ortho'*-substituted terphenyl and re-establishment of the conjugation. The radical centre is predominantly situated at the outer cyclopentadienes, most probably to retain a maximum number of fully intact benzene rings. It shows a very small triradical character and a small SOMO–LUMO gap.

Experimental

Detailed experimental procedures and spectroscopic data for all new compounds are given in the ESI.†

2,2′-[9-(2,4,6-Trimethylphenyl)-9*H*-fluorene-4,5-diyl] dibenzaldehyde (22)

PdCl$_2$(PPh$_3$)$_2$ (18 mg, 26 µmol) was added with positive argon pressure to a degassed (ultrasonication) solution of fluorene **20** (200 mg, 452 µmol), 2-(4,4,5,5-tetramethyl-1,3,2-dioxaborolan-2-yl)benzaldehyde[26] (**21**, 262 mg, 1.13 mmol), and Na$_2$CO$_3$ (220 mg, 2.06 mmol) in THF/H$_2$O (5 : 4, 9 mL), placed in a Schlenk tube. The flask was closed and the mixture was heated to 80 °C for 15 h. The mixture was cooled to rt, half-concentrated brine (5 mL) was added, and the mixture was extracted with EtOAc (3 × 15 mL). The combined organic layers were dried (Na$_2$SO$_4$), concentrated at reduced pressure, and purified by column chromatography (silica gel, hexane/EtOAc, 10 : 1) to yield **22** as a colourless solid (115 mg, 233 µmol, 52%). The

product was obtained as a mixture of atropisomers. R_f = 0.38 (hexane/EtOAc 4 : 1); IR (ATR): $\tilde{\nu}$ = 2842 (vw), 2749 (vw), 1689 (m), 1594 (w), 1447 (w), 1392 (w), 1247 (w), 1194 (w), 1159 (vw), 854 (vw), 829 (w), 757 (m), 715 (w), 644 (w), 578 (vw), 449 (vw) cm^{-1}; MS (FAB): *m/z* (%): 493.3 (16) $[M + 1]^+$, 492.3 (15) $[M]^+$, 475.3 (28), 474.3 (23); HRMS (FAB): *m/z* calcd for C$_{36}$H$_{28}$O$_2$: 492.2084 $[M^+]$; found: 492.2085.

4,8,11-Tris(2,4,6-trimethylphenyl)-8,11-dihydro-4*H*-cyclopenta [1,2-*c*:4,3-*c′*]difluorene (24)

Following a published protocol[6] MesMgBr (1 M in THF; 1.15 mL, 1.15 mmol) was added dropwise within 5 min under argon atmosphere to a cooled (0 °C) solution of fluorene **22** (115 mg, 233 µmol) in anhydrous THF (6 mL). The cooling bath was removed and the mixture was stirred for 15 min at rt. Saturated aqueous NH$_4$Cl solution (20 mL) was added, stirring was continued for 10 min, and the mixture was extracted with CH$_2$Cl$_2$ (3 × 25 mL). The combined organic layers were dried (MgSO$_4$) and concentrated at reduced pressure. The residue (**23**) was dissolved in anhydrous CH$_2$Cl$_2$ (25 mL), cooled to 0 °C, and BF$_3$·OEt$_2$ (0.15 mL, 173 mg, 1.22 mmol) was added within 5 min. Stirring was continued for 1 h at rt and saturated aqueous NH$_4$Cl solution (25 mL) was added. The mixture was stirred for 10 min and extracted with CH$_2$Cl$_2$ (2 × 20 mL). The organic layers were dried (MgSO$_4$), concentrated at reduced pressure, and purified by column chromatography (silica gel, hexane/CH$_2$Cl$_2$, 4 : 1) furnishing an oil, which was digested in CH$_2$Cl$_2$ (2 mL) and precipitated with MeOH to yield **24** as a white powder (117 mg, 167 µmol, 63%). The product was obtained as a mixture of isomers; reasonable NMR spectra could thus not be measured. R_f = 0.17 (hexane/CH$_2$Cl$_2$ 4 : 1); IR (ATR): $\tilde{\nu}$ = 2914 (vw), 1611 (vw), 1447 (w), 1401 (vw), 1377 (vw), 1342 (vw), 1016 (vw), 849 (w), 814 (vw), 774 (w), 732 (m), 709 (w), 661 (vw), 632 (vw), 551 (vw), 439 (vw) cm^{-1}; MS (FAB): *m/z* (%): 698.4 (32) $[M + 2]^+$, 697.4 (85) $[M + 1]^+$, 696.4 (100) $[M]^+$, 695.4 (34) $[M − 1]^+$, 578.3 (34), 577.3 (75) $[M − \text{Mes}]^+$, 576.3 (30), 458.2 (15) $[M − 2\text{Mes}]^+$; HRMS (FAB): *m/z* calcd for C$_{54}$H$_{48}$: 696.3751 $[M]^+$; found: 696.3752.

5,8,11-Tris(2,4,6-trimethylphenyl)cyclopenta[1,2-*c*:4,3-*c′*] difluoren-5-yl (7)

Following a published protocol[13] heptacycle **24** (100 mg, 144 µmol) and *t*BuOK (229 mg, 2.04 mmol), placed in a Schlenk tube, were dissolved under an argon atmosphere in anhydrous THF (7 mL) and the mixture was heated to 60 °C for 16 h. The mixture was cooled to rt, chloranil (160 mg, 649 µg) was added, and after a short stirring (4 min) the mixture was concentrated at reduced pressure. The residue was purified by column chromatography (silica gel, hexane/CH$_2$Cl$_2$, 4 : 1) to furnish **7** as a black solid (84 mg, 121 µmol, 84%). It was digested in degassed CHCl$_3$ (2 mL) and covered with degassed MeOH (3 mL). Slow, undisturbed diffusion yielded black, rod-shaped crystals, suitable for X-ray crystallography. R_f = 0.35 (hexane/CH$_2$Cl$_2$ 4 : 1); m.p. 241 °C (CHCl$_3$/EtOH); IR (ATR): $\tilde{\nu}$ = 2962 (w), 2914 (w), 1737 (vw), 1610 (w), 1561 (vw), 1459 (w), 1442 (w), 1376 (w), 1347 (w), 1260 (w),

2878 | *Org. Biomol. Chem.*, 2022, **20**, 2873–2880

This journal is © The Royal Society of Chemistry 2022

1189 (w), 1140 (w), 1090 (w), 1014 (w), 941 (w), 911 (vw), 847 (w), 807 (m), 793 (m), 745 (m), 692 (m), 576 (vw), 549 (w), 438 (vw) cm^{-1}; UV/Vis (CH$_2$Cl$_2$): λ_{max} (ε) = 262 (54 000), 315 (33 000), 348 (22 000), 449 (27 000), 769 (6000), 855 nm (12 000 mol^{-1} dm^3 cm^{-1}); MS (FAB): m/z (%): 694.4 (20) $[M + 1]^+$, 693.4 (19) $[M]^+$; HRMS (FAB): m/z calcd for C$_{54}$H$_{45}$: 693.3516 $[M]^+$; found: 693.3518.

Author contributions

S. H. and J. P. designed the project, S. H. performed the syntheses and measured NMR, IR, and MS spectra. A. H. performed the XRD analysis, J. P. did the quantum chemical calculations, A. H. and F. B. measured and analysed EPR spectra and the cyclic voltammograms. All authors contributed to the interpretation of the results. S. H. and J. P. prepared the manuscript with input from all contributing authors.

Conflicts of interest

There are no conflicts to declare.

Acknowledgements

Notes and references

1 (a) D. Hellwinkel and G. Reiff, *Angew. Chem.*, 1970, **82**, 516–517, (*Angew. Chem., Int. Ed. Engl.*, 1970, **9**, 527–528); (b) D. Hellwinkel, G. Reiff and V. Nykodym, *Justus Liebigs Ann. Chem.*, 1977, 1013–1025; (c) S. Marković, J. Đurđević, S. Jeremić and I. Gutman, *J. Serb. Chem. Soc.*, 2010, **75**, 1241–1249; (d) H. Hopf, *Angew. Chem.*, 2013, **125**, 12446–12449, (*Angew. Chem., Int. Ed.*, 2013, **52**, 12224–12226); (e) S. Das and J. Wu, in *Polycyclic Arenes and Heteroarenes: Synthesis, Properties, and Applications*, ed. Q. Miao, Weinheim-VCH, Weinheim, 2015, pp. 1–36; (f) P. Hu, S. Lee, T. S. Herng, N. Aratani, T. P. Gonçalves, Q. Qi, X. Shi, H. Yamada, K.-W. Huang, J. Ding, D. Kim and J. Wu, *J. Am. Chem. Soc.*, 2016, **138**, 1065–1077; (g) X. Yang, X. Shi, N. Aratani, T. P. Gonçalves, K.-W. Huang, H. Yamada, C. Chi and Q. Miao, *Chem. Sci.*, 2016, **7**, 6176–6181; (h) C. K. Frederickson, L. N. Zakharov and M. M. Haley, *J. Am. Chem. Soc.*, 2016, **138**, 16827–16838; (i) S. Das and J. Wu, *Phys. Sci. Rev.*, 2017, **2**, 20160109; (j) K. Yamamoto, Y. Ie, N. Tohnai, F. Kakiuchi and Y. Aso, *Sci. Rep.*, 2018, **8**, 17663; (k) T. Jousselin-Oba, P. E. Deal, A. G. Fix, C. K. Frederickson, C. L. Vonnegut, A. Yassar, L. N. Zakharov, M. Frigoli and M. M. Haley, *Chem. – Asian J.*, 2019, **14**, 1737–1744; (l) H. Miyoshi, I. Hisaki and Y. Tobe, *Eur. J. Org. Chem.*, 2021, 3528–3534; (m) Q. Chen, M. Baumgarten, M. Wagner, Y. Hu, I. C.-Y. Hou, A. Narita and K. Müllen, *Angew. Chem.*, 2021, **133**, 11400–11404, (*Angew. Chem., Int. Ed.*, 2021, **60**, 11300–11304); (n) J. R. Dias, *J. Phys. Chem. A*, 2021, **125**, 8482–8497, (*J. Phys. Chem. A*, 2021, **125**, 9940); (o) T. Xu, Y. Han, Z. Shen, X. Hou, Q. Jiang, W. Zeng, P. W. Ng and C. Chi, *J. Am. Chem. Soc.*, 2021, **143**, 20562–20568.

2 (a) G. E. Rudebusch and M. M. Haley, in *Polycyclic Arenes and Heteroarenes: Synthesis, Properties, and Applications*, ed. Q. Miao, Wiley-VCH, Weinheim, 2015, pp. 37–60; (b) J. Ma, J. Liu, M. Baumgarten, Y. Fu, Y.-Z. Tan, K. S. Schellhammer, F. Ortmann, G. Cuniberti, H. Komber, R. Berger, K. Müllen and X. Feng, *Angew. Chem.*, 2017, **129**, 3328–3332, (*Angew. Chem., Int. Ed.*, 2017, **56**, 3280–3284).

3 (a) Y. Tobe, *Chem. Rec.*, 2015, **15**, 86–96; (b) A. Konishi and M. Yasuda, *Chem. Lett.*, 2021, **50**, 195–212.

4 (a) A. Shimizu and Y. Tobe, *Angew. Chem.*, 2011, **123**, 7038–7042; *Angew. Chem., Int. Ed.*, 2011, **50**, 6906–6910; (b) Y. Tobe and T. Kubo, in *Top. Curr. Chem*, Springer, Cham, 2018; (c) J. Guo, Z. Li, J. Zhang, B. Li, Y. Liang, Y. Wang, S. Xie, H. Phan, T. S. Herng, J. Ding, J. Wu, B. Z. Tang and Z. Zeng, *CCS Chem.*, 2021, **3**, 399–407.

5 (a) A. G. Fix, D. T. Chase and M. M. Haley, in *Polyarenes I*, ed. J. S. Siegel and Y.-T. Wu, Springer, Berlin, Heidelberg, 2014, pp. 159–195; (b) C. K. Frederickson, B. D. Rose and M. M. Haley, *Acc. Chem. Res.*, 2017, **50**, 977–987.

6 H. Sharma, P. K. Sharma and S. Das, *Chem. Commun.*, 2020, **56**, 11319–11322.

7 (a) E. Clar, in *Polycyclic Hydrocarbons*, Academic Press, London, Springer-Verlag, Berlin, 1964, vol. 1, pp. 32–39; (b) A. D. Zdetsis, *J. Phys. Chem. C*, 2018, **122**, 17526–17536; (c) Y. Wang, *J. Phys. Chem. A*, 2022, **126**, 164–176.

8 (a) E. Font-Sanchis, C. Aliaga, E. V. Bejan, R. Cornejo and J. C. Scaiano, *J. Org. Chem.*, 2003, **68**, 3199–3204; (b) L. E. Harrington, J. F. Britten and M. J. McGlinchey, *Tetrahedron Lett.*, 2003, **44**, 8057–8060.

9 (a) R. C. Gostowski, T. Bailey, S. D. Bonner, E. E. Emrich and S. L. Steelman, *J. Phys. Org. Chem.*, 2000, **13**, 735–739; (b) Y. Tian, K. Uchida, H. Kurata, Y. Hirao, T. Nishiuchi and T. Kubo, *J. Am. Chem. Soc.*, 2014, **136**, 12784–12793; (c) D. T. Hogan and T. C. Sutherland, *J. Phys. Chem. Lett.*, 2018, **9**, 2825–2829; (d) T. Nishiuchi, R. Ito, A. Takada, Y. Yasuda, T. Nagata, E. Stratmann and T. Kubo, *Chem, – Asian J.*, 2019, **14**, 1830–1836.

10 (a) C. Poriel, J.-J. Liang, J. Rault-Berthelot, F. Barrière, N. Cocherel, A. M. Z. Slawin, D. Horhant, M. Virboul, G. Alcaraz, N. Audebrand, L. Vignau, N. Huby, G. Wantz and L. Hirsch, *Chem. – Eur. J.*, 2007, **13**, 10055–10069; (b) H. Usta, A. Facchetti and T. J. Marks, *J. Am. Chem. Soc.*, 2008, **130**, 8580–8581; (c) H. Usta, C. Risko, Z. Wang, H. Huang, M. K. Deliomeroglu, A. Zhukhovitskiy, A. Facchetti and T. J. Marks, *J. Am. Chem. Soc.*, 2009, **131**, 5586–5608; (d) D. T. Chase, A. G. Fix, S. J. Kang, B. D. Rose,

This journal is © The Royal Society of Chemistry 2022

Org. Biomol. Chem., 2022, **20**, 2873–2880 | **2879**

C. D. Weber, Y. Zhong, L. N. Zakharov, M. C. Lonergan, C. Nuckolls and M. M. Haley, *J. Am. Chem. Soc.*, 2012, **134**, 10349–10352; (*e*) X. Yang, D. Liu and Q. Miao, *Angew. Chem.*, 2014, **126**, 6904–6908, (*Angew. Chem., Int. Ed.*, 2014, **53**, 6786–6790).

11 K. Fukuda, J.-y. Fujiyoshi, H. Matsui, T. Nagami, S. Takamuku, Y. Kitagawa, B. Champagne and M. Nakano, *Org. Chem. Front.*, 2017, **4**, 779–789.

12 (*a*) K. Kamada, K. Ohta, A. Shimizu, T. Kubo, R. Kishi, H. Takahashi, E. Botek, B. Champagne and M. Nakano, *J. Phys. Chem. Lett.*, 2010, **1**, 937–940; (*b*) S. Nobusue, H. Miyoshi, A. Shimizu, I. Hisaki, K. Fukuda, M. Nakano and Y. Tobe, *Angew. Chem.*, 2015, **127**, 2118–2122, (*Angew. Chem., Int. Ed.*, 2015, **54**, 2090–2094); (*c*) C. Liu, Y. Ni, X. Lu, G. Li and J. Wu, *Acc. Chem. Res.*, 2019, **52**, 2309–2321; (*d*) Q. Jiang, Y. Han, Y. Zou, H. Phan, L. Yuan, T. S. Herng, J. Ding and C. Chi, *Chem. – Eur. J.*, 2020, **26**, 15613–15622.

13 X. Yang, D. Zhang, Y. Liao and D. Zhao, *J. Org. Chem.*, 2020, **85**, 5761–5770.

14 (*a*) T. Kubo, K. Yamamoto, K. Nakasuji, T. Takui and I. Murata, *Angew. Chem.*, 1996, **108**, 456–457, (*Angew. Chem., Int. Ed. Engl.*, 1996, **35**, 439–441); (*b*) T. Kubo, K. Yamamoto, K. Nakasuji, T. Takui and I. Murata, *Bull. Chem. Soc. Jpn.*, 2001, **74**, 1999–2009; (*c*) R. G. Hicks, *Org. Biomol. Chem.*, 2007, **5**, 1321–1338; (*d*) Y. Morita and S. Nishida, in *Stable Radicals: Fundamentals and Applied Aspects of Odd-Electron Compounds*, ed. R. G. Hicks, John Wiley & Sons, Chichester, 2010, pp. 81–145; (*e*) T. Kubo, Y. Katada, A. Shimizu, Y. Hirao, K. Sato, T. Takui, M. Uruichi, K. Yakushi and R. C. Haddon, *J. Am. Chem. Soc.*, 2011, **133**, 14240–14243; (*f*) M. Abe, *Chem. Rev.*, 2013, **113**, 7011–7088; (*g*) B. Prajapati, D.-K. Dang, P. J. Chmielewski, M. A. Majewski, T. Lis, C. J. Gómez-García, P. M. Zimmerman and M. Stępień, *Angew. Chem.*, 2021, **133**, 22670–22678, (*Angew. Chem., Int. Ed.*, 2021, **60**, 22496–22504).

15 (*a*) H. Nishide and K. Oyaizu, *Science*, 2008, **319**, 737–738; (*b*) Y. Morita, S. Nishida, T. Murata, M. Moriguchi, A. Ueda, M. Satoh, K. Arifuku, K. Sato and T. Takui, *Nat. Mater.*, 2011, **10**, 947–951.

16 R. G. Hicks, in *Stable radicals: fundamentals and applied aspects of odd-electron compounds*, ed. R. G. Hicks, Wiley, Chichester, 2010, pp. 317–380.

17 G. P. Moss, P. A. S. Smith and D. Tavernier, *Pure Appl. Chem.*, 1995, **67**, 1307–1375.

18 H. A. Favre and W. H. Powell, *Nomenclature of Organic Chemistry: IUPAC Recommendations and Preferred Names 2013*, The Royal Society of Chemistry, 2013.

19 T. Cadart, D. Nečas, R. P. Kaiser, L. Favereau, I. Císařová, R. Gyepes, J. Hodačová, K. Kalíková, L. Bednárová, J. Crassous and M. Kotora, *Chem. – Eur. J.*, 2021, **27**, 11279–11284.

20 B. M. Gross and M. Oestreich, *Synthesis*, 2021, **53**, 2512–2516.

21 A. Weiß and J. Podlech, *Eur. J. Org. Chem.*, 2019, 6697–6701.

22 A. G. Fix, P. E. Deal, C. L. Vonnegut, B. D. Rose, L. N. Zakharov and M. M. Haley, *Org. Lett.*, 2013, **15**, 1362–1365.

23 D. C. Ebner, J. T. Bagdanoff, E. M. Ferreira, R. M. McFadden, D. D. Caspi, R. M. Trend and B. M. Stoltz, *Chem. – Eur. J.*, 2009, **15**, 12978–12992.

24 P. E. Eaton, G. R. Carlson and J. T. Lee, *J. Org. Chem.*, 1973, **38**, 4071–4073.

25 (*a*) Y. Miyake, M. Wu, M. J. Rahman, Y. Kuwatani and M. Iyoda, *J. Org. Chem.*, 2006, **71**, 6110–6117; (*b*) Q. Perron, J. Praz and A. Alexakis, *Tetrahedron: Asymmetry*, 2009, **20**, 1004–1007; (*c*) Q. Perron and A. Alexakis, *Adv. Synth. Catal.*, 2010, **352**, 2611–2620.

26 Y.-Y. Jhang, T.-T. Fan-Chiang, J.-M. Huang and J.-C. Hsieh, *Org. Lett.*, 2016, **18**, 1154–1157.

27 S. Stoll and A. Schweiger, *J. Magn. Reson.*, 2006, **178**, 42–55.

28 (*a*) J. Kruszewski and T. M. Krygowski, *Tetrahedron Lett.*, 1972, **13**, 3839–3842; (*b*) T. M. Krygowski, *J. Chem. Inf. Comput. Sci.*, 1993, **33**, 70–78; (*c*) T. M. Krygowski and M. K. Cyrański, *Chem. Rev.*, 2001, **101**, 1385–1420.

29 (*a*) J. A. N. F. Gomes and R. B. Mallion, *Chem. Rev.*, 2001, **101**, 1349–1383; (*b*) Z. Chen, C. S. Wannere, C. Corminboeuf, R. Puchta and P. v. R. Schleyer, *Chem. Rev.*, 2005, **105**, 3842–3888; (*c*) A. Stanger, *J. Org. Chem.*, 2006, **71**, 883–893; (*d*) H. Fallah-Bagher-Shaidaei, C. S. Wannere, C. Corminboeuf, R. Puchta and P. v. R. Schleyer, *Org. Lett.*, 2006, **8**, 863–866; (*e*) A. Stanger, *Eur. J. Org. Chem.*, 2020, 3120–3127.

30 R. H. Mitchell, *Chem. Rev.*, 2001, **101**, 1301–1315.

31 K. H. Hausser, H. Brunner and J. C. Jochims, *Mol. Phys.*, 1966, **10**, 253–260.

32 (*a*) J. Pommerehne, H. Vestweber, W. Guss, R. F. Mahrt, H. Bässler, M. Porsch and J. Daub, *Adv. Mater.*, 1995, **7**, 551–554; (*b*) C. M. Cardona, W. Li, A. E. Kaifer, D. Stockdale and G. C. Bazan, *Adv. Mater.*, 2011, **23**, 2367–2371; (*c*) J. Sworakowski, *Synth. Met.*, 2018, **235**, 125–130; (*d*) E. V. Tretyakov, P. V. Petunin, S. I. Zhivetyeva, D. E. Gorbunov, N. P. Gritsan, M. V. Fedin, D. V. Stass, R. I. Samoilova, I. Y. Bagryanskaya, I. K. Shundrina, A. S. Bogomyakov, M. S. Kazantsev, P. S. Postnikov, M. E. Trusova and V. I. Ovcharenko, *J. Am. Chem. Soc.*, 2021, **143**, 8164–8176.

33 D. Döhnert and J. Koutecký, *J. Am. Chem. Soc.*, 1980, **102**, 1789–1796.

34 K. Yamaguchi, *Chem. Phys. Lett.*, 1975, **33**, 330–335.

35 (*a*) F. Cervantes-Navarro and D. Glossman-Mitnik, *J. Mex. Chem. Soc.*, 2013, **57**, 19–22; (*b*) J. Podlech, S. C. Fleck, M. Metzler, J. Bürck and A. S. Ulrich, *Chem. – Eur. J.*, 2014, **20**, 11463–11470.

2880 | *Org. Biomol. Chem.*, 2022, **20**, 2873–2880

This journal is © The Royal Society of Chemistry 2022